

Deployment-friendly Lane-changing Intention Prediction Powered by Brain-inspired Spiking Neural Networks

1st Shuqi Shen

*The Hong Kong University of
Science and Technology (Guangzhou)*
Guangzhou, China
u202141021@xs.ustb.edu.cn

1st Junjie Yang

*The Hong Kong University of
Science and Technology (Guangzhou)*
Guangzhou, China
jyang512@connect.hkust-gz.edu.cn

3rd Hui Zhong

*The Hong Kong University of
Science and Technology (Guangzhou)*
Guangzhou, China
hzhong638@connect.hkust-gz.edu.cn

4th Hongliang Lu*

*The Hong Kong University of
Science and Technology (Guangzhou)*
Guangzhou, China
hlu592@connect.hkust-gz.edu.cn

*Corresponding author

5th Xinhua Zheng*

*The Hong Kong University of
Science and Technology (Guangzhou)*
Guangzhou, China
xinhuzheng@hkust-gz.edu.cn

*Corresponding author

6th Hai Yang

*The Hong Kong University of
Science and Technology*
Hongkong, China
cehyang@ust.hk

Abstract—Accurate and real-time prediction of surrounding vehicles’ lane-changing intentions is a critical challenge in deploying safe and efficient autonomous driving systems in open-world scenarios. Existing high-performing methods remain hard to deploy due to their high computational cost, long training times, and excessive memory requirements. Here, we propose an efficient lane-changing intention prediction approach based on brain-inspired Spiking Neural Networks (SNN). By leveraging the event-driven nature of SNN, the proposed approach enables us to encode the vehicle’s states in a more efficient manner. Comparison experiments conducted on HighD and NGSIM datasets demonstrate that our method significantly improves training efficiency and reduces deployment costs while maintaining comparable prediction accuracy. Particularly, compared to the baseline, our approach reduces training time by 75% and memory usage by 99.9%. These results validate the efficiency and reliability of our method in lane-changing predictions, highlighting its potential for safe and efficient autonomous driving systems while offering significant advantages in deployment, including reduced training time, lower memory usage, and faster inference.

Index Terms—Lane-changing intention prediction, Spiking Neural Networks (SNN), autonomous driving, real-time prediction, HighD dataset, NGSIM dataset.

I. INTRODUCTION

In the field of autonomous driving, the rapid and accurate prediction of lane-changing intentions of surrounding vehicles is critical for enhancing system safety and decision-making efficiency. Precise intention prediction can not only effectively prevent potential collisions but also optimize path planning and traffic flow management, resulting in a smarter and more efficient driving experience [1].

Recent advancements in lane-changing prediction research have been remarkable. Unlike earlier approaches that relied on physical models that simulate vehicle dynamics through predefined mathematical equations [2], [3], modern research has shifted toward learning-based methods. For instance, back-propagation neural networks effectively predict lane-changing intentions by learning from real-world data [4]. Similarly, temporal models such as Long Short-Term Memory (LSTM) networks have gained popularity for their ability to capture temporal dependencies in lane-changing prediction tasks [5]. The Echo State Network (ESN), a more recent temporal model, further improves prediction performance through its unique dynamic properties [6]. Learning-based methods for lane-changing prediction, despite their advancements, face notable limitations. They require extensive training data, involve prolonged training durations, and demand significant hardware resources, posing challenges for real-time deployment on onboard devices. These issues highlight the need for more efficient and lightweight solutions [7]. Furthermore, the continuous influx of massive amounts of data amplifies the need for fast algorithm iterations and real-time processing capabilities. As a result, lane-changing prediction algorithms must balance efficient training, rapid deployment, and real-time reliability to meet the demands of practical applications.

Brain-inspired computational methods have recently made groundbreaking progress. SNN, known as the third-generation neural network [8], exhibits unique advantages

in intelligent embedded systems due to biological interpretability and deployment efficiency. Unlike traditional Artificial Neural Networks (ANN), SNN is event-driven, relying on a sparse spike timing encoding mechanism to process information. This event-driven feature enhances computational energy efficiency by 12 times, as it only processes information when events occur, reducing unnecessary computation cost [9]. Therefore, numerous researchers have shown great interest in SNN. [10] introduced the surrogate gradient method into SNN, significantly improving training speed by over threefold, while also enhancing deployment efficiency. [11] developed an ANN-SNN conversion framework, which maintained model accuracy while increasing training efficiency by 75%, and also reduced resource consumption. These researches collectively highlight the significant potential of SNN in achieving both high computational and deployment efficiency and reliable performance, making SNN a promising solution for future real-world practical applications.

In this paper, we propose an efficient lane-changing intention prediction method based on brain-inspired SNN. Specifically, our approach first utilizes a linear layer to feature the vehicle's driving state. Then, we employ SNN to understand and predict the vehicle's lane-changing intention in real-time, categorizing it into no lane-keeping, turn left, or turn right. To evaluate our approach, several groups of comparison experiments are carried out. we utilize two open-source naturalistic driving datasets, HighD [12] and NGSIM [13], to assess the performance in terms of efficiency and accuracy. The advantages of SNN in resource consumption support the development of highly efficient algorithms and seamless hardware deployment, enabling scalable and practical autonomous driving solutions. Looking ahead, brain-inspired approaches like SNN stand out as a key advantage for autonomous driving, offering a paradigm shift in mimicking the brain's adaptive and efficient problem-solving capabilities.

The remainder of this paper is organized as follows. Section II discusses the related work. Section III introduces the proposed methodology in detail. Section IV presents the experimental results and analyzes the findings. Finally, Section V concludes the paper and highlights potential directions for future research.

II. RELATED WORK

This section reviews previous work on lane-changing prediction and SNN. We first discuss the development of lane-changing prediction methods, comparing kinematic or kinetic models and behavioral models with learning-based approaches, and highlight their limitations. Next, we introduce SNN, emphasizing its advantages and applications, particularly in traffic and autonomous vehicle domains.

A. Lane-Changing Intention Prediction

Lane-changing prediction refers to predicting whether and when other vehicles will execute a lane change in a traffic environment. Early lane-changing prediction approaches were

primarily based on kinematic or kinetic models, typically using mathematical formulas for modeling. For example, [14] used polar coordinate polynomials to fit vehicle trajectories and predict their motion, demonstrating an effective mathematical approach for trajectory prediction. Non-linear dynamic models and model predictive control were utilized to ensure longitudinal safety and lateral stability in lane-changing scenarios, showcasing their potential in maintaining vehicle control under various conditions [15]. Besides, behavioral modeling methods were also widely utilized. For example, [16] modeled the driver's decision-making process and improved lane-changing prediction accuracy by explicitly selecting target lanes and evaluating lane-change safety. These models achieve high prediction accuracy by relying heavily on their complexity, however, the computational demands make them unsuitable for resource-constrained onboard deployment in real-time applications. In recent years, learning-based methods have gradually become the mainstream in lane-changing prediction. For example, [17] employed a multilayer perceptron to learn driving trajectories and predict lane changes, demonstrating the potential of neural networks for capturing lane-changing patterns. Similarly, the combination of bidirectional RNN and LSTM proved effective for predicting highway lane-changing intentions using time-series driving data, showcasing the strength of temporal models in handling sequential information [18]. [19] advanced lane-changing prediction by applying ESN and Principal Component Analysis to naturalistic driving data, leveraging driver-specific data for precision. Additionally, [20] introduced an online transfer learning approach that efficiently predicted lane-changing intentions even with limited data, expanding the applicability of learning-based methods in diverse scenarios. Overall, these learning-based methods fail to achieve both efficient training and deployment and high prediction accuracy at the same time. Therefore, a deployment-friendly approach for efficient lane-changing intention prediction is needed.

B. Spiking Neural Networks

SNN are efficient, low-power, and biologically interpretable neural networks that are particularly suited for processing time-series data and real-time applications in resource-constrained environments. In recent years, SNN have been widely applied in many fields. For example, [21] utilized SNN for time series classification and designed a sparse spatiotemporal spike encoding scheme and training algorithm, achieving classification performance comparable to deep neural networks under low-power conditions. [22] utilized SNN for dynamic vision sensing (DVS) optimization tasks, achieving optimal performance for deep SNN across multiple benchmark datasets. [23] used SNN for visual recognition tasks and demonstrated superior performance on SNN-specific datasets with a significant reduction in energy consumption. [24] proposed a new ANN-SNN conversion mechanism for complex visual recognition tasks that ensured recognition accuracy and significantly improved training efficiency. In the field of transportation, SNN have also gar-

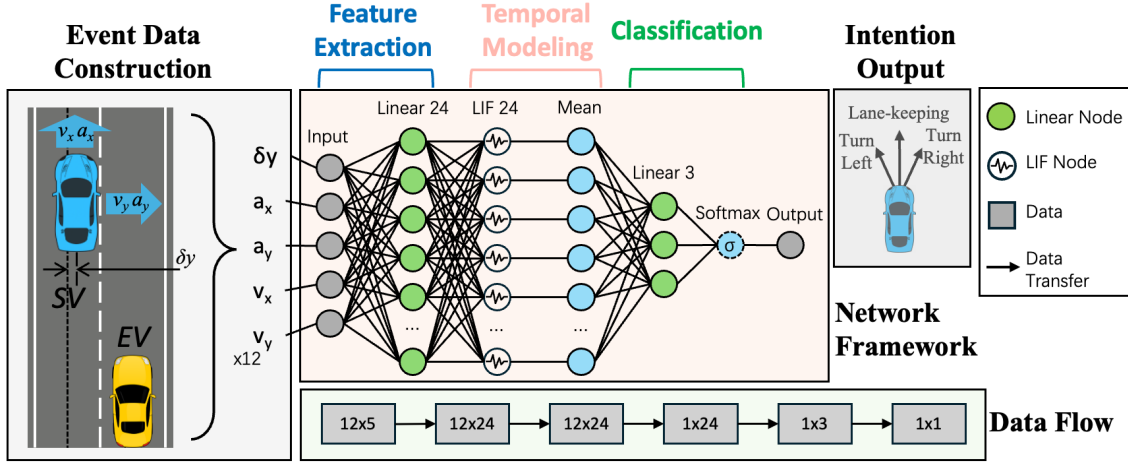


Fig. 1. Schematic of the SNN model for lane-changing intention prediction. The model processes a time-series input of vehicle state features through four main components: (1) Event Data Construction to generate the input matrix, (2) Feature Extraction with a Linear layer to expand feature dimensions, (3) Temporal Modeling using a LIF layer to capture temporal dependencies, and (4) Classification where a Linear layer maps the features to lane-change intention categories, followed by a Softmax activation for prediction.

nered significant attention. In the classification tasks of other traffic participants, the combination of SNN and event-based cameras demonstrated efficient classification capabilities with low power consumption and low latency [25]. [26] proposed novel SNN for AV radar signal processing, which achieved efficient processing performance and maintained low power consumption in simulated driving scenarios. [27] applied SNN to lane-keeping tasks to achieve fast learning, which improved positioning accuracy and significantly reduced computational energy consumption. In summary, SNN has shown great promise in transportation applications, meeting the critical demands of autonomous driving for fast, energy-efficient deployment.

III. METHODOLOGY

This section introduces the proposed approach for efficient lane-changing intention prediction using SNN, including the network architecture and the training process.

A. Proposed SNN Architecture

To capture the temporal dynamics in lane-changing processes, we propose a model based on Spiking Neural Networks (SNN), as illustrated in Figure 1. The input to the model consists of a time-series matrix representing vehicle state features with dimensions $(12, 5)$. Each row corresponds to a time step, and the five feature dimensions include lateral distance to the lane center (δ_y), longitudinal velocity (v_x), longitudinal acceleration (a_x), lateral velocity (v_y), and lateral acceleration (a_y). These features provide critical spatial and dynamic information required for understanding lane-changing behavior. During dataset construction, lane-changing initiation is defined as the moment when the vehicle starts deviating from its lane. It is assumed that drivers form clear lane-changing intentions 3 s before this moment [28].

The model architecture integrates three main components to enable efficient and accurate prediction of lane-changing

intentions. First, the feature extraction module, implemented as a Linear layer, expands the input feature dimensions, enhancing the representation power of the data. Next, the temporal modeling module, implemented as a Leaky Integrate-and-Fire (LIF) layer, captures the dynamic dependencies in the input data by simulating biological neuron behaviors. Finally, the classification module aggregates the extracted temporal features and maps them into a probabilistic output representing three categories of lane-changing intentions. This architecture ensures that the temporal patterns in the input data are preserved and efficiently processed, enabling accurate predictions while maintaining computational efficiency.

B. Model Training

The training process involves detailed data transformations and computations within each component of the model. The input to the model is a time-series matrix $\mathbf{X} \in \mathbb{R}^{[12,5]}$ of vehicle state features, which first undergoes a feature expansion step through a linear layer. This layer transforms the input dimensions from $(12, 5)$ to a $(12, 24)$ matrix $\mathbf{I} \in \mathbb{R}^{[12,24]}$ by applying a linear transformation:

$$\mathbf{I} = \mathbf{X}\mathbf{W} + \mathbf{b} \quad (1)$$

where \mathbf{W} and \mathbf{b} are the weight matrix and bias vector of the linear layer. This expansion improves the expressive power of the features.

The expanded feature matrix is then processed by the LIF layer, which models temporal dependencies using a neuron state update mechanism. Each neuron processes a specific feature dimension independently, with its state updated iteratively across time steps:

$$u_j[t] = \beta \cdot u_j[t-1] + I[t, j] \quad (2)$$

where $\beta \in (0, 1)$ is the decay coefficient that controls the retention of historical states. When the neuron's state exceeds a predefined threshold, it emits a spike, resetting its state:

$$s_j[t] = \begin{cases} 1, & u_j[t] \geq V_{th} \\ 0, & \text{otherwise} \end{cases} \quad (3)$$

The output of the LIF layer is a spike matrix $\mathbf{S} \in 0, 1^{[12, 24]}$. To extract global temporal features, the spike matrix is averaged along the time dimension:

$$\bar{S}_j = \frac{1}{12} \sum_{t=1}^{12} S_j[t], \quad \forall j \in 1, \dots, 24 \quad (4)$$

This produces a $(1, 24)$ feature vector, which is then passed through a linear layer that maps the features to a 3-dimensional output corresponding to the three lane-changing intention categories. Finally, a Softmax activation function is applied to convert the outputs into a probability distribution:

$$P_i = \frac{\exp(z_i)}{\sum_{k=1}^3 \exp(z_k)}, \quad i \in 0, 1, 2 \quad (5)$$

where z_i is the i_{th} output, and P_i represents the predicted probability of the i_{th} lane-changing intention.

The model is trained using supervised learning, with the goal of minimizing the difference between the predicted probability distribution and the true labels. Negative log-likelihood loss (NLLLoss) is used as the loss function:

$$\mathcal{L} = -\frac{1}{N} \sum_{i=1}^N \log P(a_t^{(i)} | s_t^{(i)}) \quad (6)$$

where $a_t^{(i)}$ represents the true lane-changing intention at time step t for the i_{th} sample, and $s_t^{(i)}$ is the corresponding input state. $P(a_t | s_t)$ denotes the predicted probability of the true class, and N is the batch size, set to 128 in this study.

Through iterative optimization, the model learns to effectively capture the dynamic patterns in vehicle state features, leading to improved performance in lane-changing intention prediction tasks.

IV. EXPERIMENTAL RESULT

This section presents the experimental results to evaluate the effectiveness and efficiency of the proposed SNN-based lane-changing intention prediction model in comparison with the ESN method and LSTM method. We train our model on HighD and NGSIM datasets, and the evaluation is conducted from three perspectives: training performance, two sample cases, and overall evaluation. All experiments, including model training and testing, are conducted on an Apple M2 CPU. First, we analyze the model's training process by comparing the time required per epoch and loss, demonstrating the superior efficiency of our approach. Second, we evaluate the model's practical application in specific scenarios, showing that our predictions align closely with the ground truth lane-changing moments, outperforming baseline methods in dynamic traffic environments. Finally, an overall evaluation is presented, highlighting the performance of our method compared to ESN and LSTM.

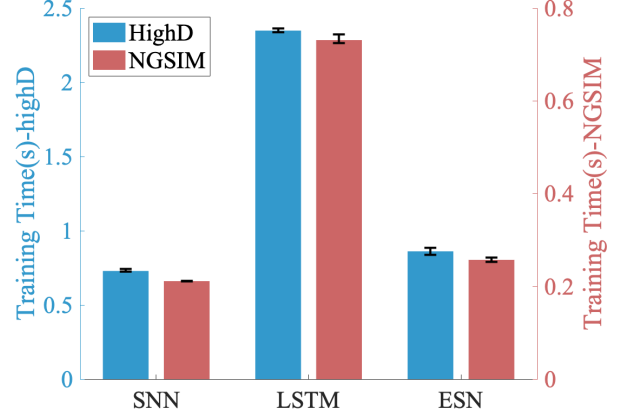


Fig. 2. Comparison of average training time per epoch for our approach, LSTM, and ESN on the HighD and NGSIM datasets.

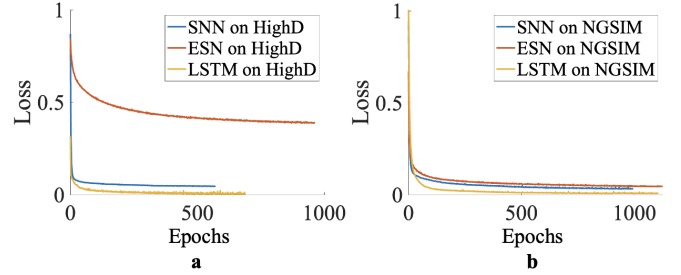


Fig. 3. Loss curves for SNN, ESN, and LSTM on the HighD (a) and NGSIM (b) datasets

A. Model Training

In this section, we present the training performance of our approach, ESN, and LSTM methods, including the training time and the loss curve. We train the models of the three approaches on the full HighD and NGSIM datasets.

First, we present the training time performance. We train the three models on the HighD and NGSIM datasets for 500 epochs and show the training time results, as shown in Figure 2. The blue axis represents the training time on the HighD dataset, while the red axis represents the training time on the NGSIM dataset. The bar chart illustrates the average training time per epoch across 500 epochs, with the blue bars representing the HighD dataset and the red bars representing the NGSIM dataset. The error bars indicate the maximum and minimum training times. On the HighD dataset, our approach achieves an average training time of 0.72 s per epoch, compared to 2.38 s for LSTM and 0.84 s for ESN. On the NGSIM dataset, our approach achieves 0.211 s per epoch, compared to 0.731 s for LSTM and 0.257 s for ESN. These results demonstrate that our approach significantly outperforms LSTM in training efficiency and slightly outperforms ESN, particularly on the NGSIM dataset.

Next, we present the loss curves of the models. During training, we stop when the loss value does not decrease within 50 epochs. As shown in Figure 3, the horizontal axis represents the number of training epochs, and the vertical

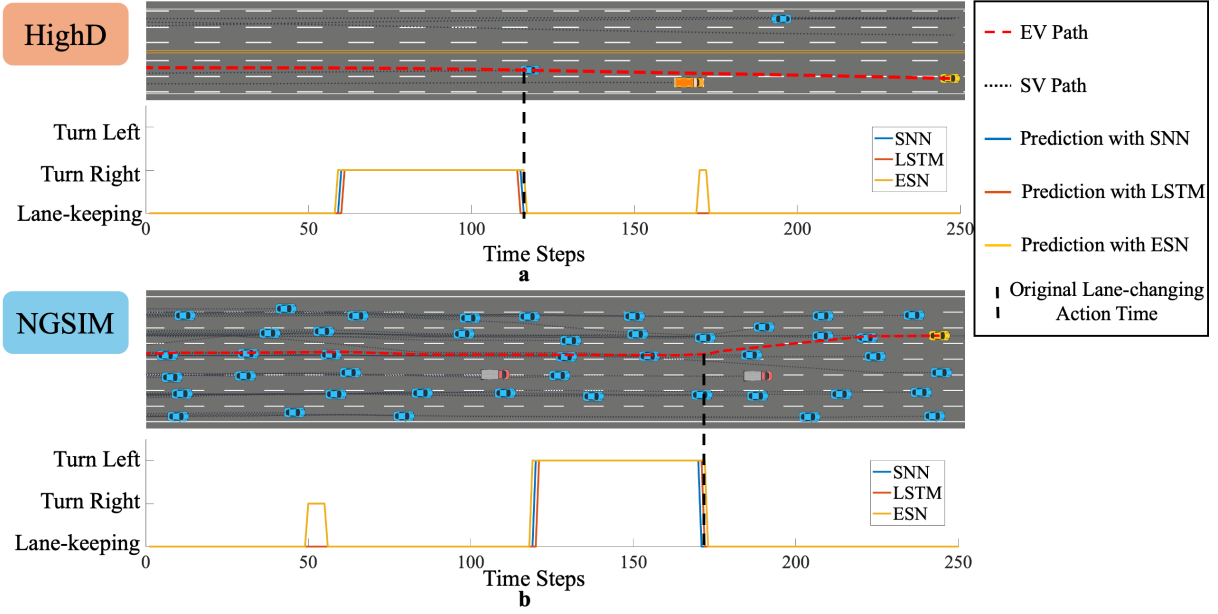


Fig. 4. Comparison of lane-changing intention predictions for SNN, LSTM, and ESN models in the HighD (a) and NGSIM (b) datasets. The blue, red, and yellow curves represent predictions from the SNN, LSTM, and ESN models, respectively. Our method predicts lane-changing accurately, with no false predictions.

axis represents the loss value. The blue curve represents our method, the red curve represents the ESN method, and the yellow curve represents the LSTM method. Figure 3a shows the loss curves for the three methods on the HighD dataset. Our method converges at 0.045 after 522 epochs, while the ESN method converges at 0.387 after 912 epochs, and the LSTM method converges at 0.0015 after 639 epochs. Figure 3b shows the loss curves on the NGSIM dataset. Our method converges at 0.032 after 945 epochs, the ESN method converges at 0.044 after 1076 epochs, and the LSTM method converges at 0.0 after 1090 epochs. The results indicate that our method achieves significantly faster convergence on the HighD dataset compared to ESN and LSTM. On the NGSIM dataset, although our method requires more epochs to converge than ESN, the final loss value is comparable to LSTM and significantly better than ESN.

In summary, our method performs exceptionally well in training efficiency. Compared to the LSTM method, our method shows a significant advantage in training time while achieving comparable loss convergence performance. Compared to the ESN method, our method demonstrates superior performance in both loss convergence and training time. These results highlight the potential of our method to achieve efficient training and excellent performance simultaneously.

B. Two Sample Cases

This section illustrates the deployment performance of our SNN model compared to the ESN and LSTM models in the HighD and NGSIM scenarios through two sample cases. The analysis includes scenario visualizations and lane-changing intention prediction curves. In Figure 4, the selected vehicles are highlighted in yellow, with their trajectories represented by red dashed lines. Other vehicles are marked

with different colors, and their trajectories are represented by black dotted lines. The lane-changing intention prediction curves are shown, with black dashed lines indicating the lane-changing moments in the original data. The blue curve represents the predictions of our method, while the red and yellow curves represent the predictions from the LSTM and ESN methods, respectively.

Figure 4a shows a scenario from the HighD dataset, where a vehicle turns right at time-step 115. Experimental results show that the proposed method predicts the lane-changing intention at time-step 60, the LSTM method at time-step 61, and the ESN method at time-step 59. However, the ESN method makes a false prediction at time-step 170. Figure 4b shows a scenario from the NGSIM dataset, where a vehicle turns left at time-step 170. Experimental results show that the proposed method predicts the lane-changing intention at time-step 120, the LSTM method at time-step 121, and the ESN method at time-step 119. However, the ESN method produces a significant false prediction at time-step 50.

In summary, the comparative experiments demonstrate that the proposed method performs exceptionally well in lane-changing intention prediction tasks. Our method produces no false predictions and maintains stable performance across different datasets and scenarios. These results confirm the effectiveness and reliability of the proposed method in practical applications.

C. Overall Evaluation

This section presents the overall performance of our method compared to ESN and LSTM, including Receiver Operating Characteristic (ROC) curves and a summary table of the overall results. The ROC curves in Figure 5 illustrate the prediction accuracy [29]. Table I summarizes the results

in terms of parameters, memory usage, training time, and accuracy.

First, Figure 5 presents the accuracy results of the three methods. The horizontal axis represents the False Positive Rate (FPR), which is the proportion of negative samples incorrectly predicted as positive. The FPR is calculated as:

$$\text{FPR} = \frac{\text{FP}}{\text{FP} + \text{TN}} \quad (7)$$

where FP (False Positive) is the number of negative samples incorrectly predicted as positive, and TN (True Negative) is the number of negative samples correctly predicted as negative. The vertical axis represents the True Positive Rate (TPR), which is the proportion of positive samples correctly predicted as positive. The TPR is calculated as:

$$\text{TPR} = \frac{\text{TP}}{\text{TP} + \text{FN}} \quad (8)$$

where TP (True Positive) is the number of positive samples correctly predicted as positive, and FN (False Negative) is the number of positive samples incorrectly predicted as negative.

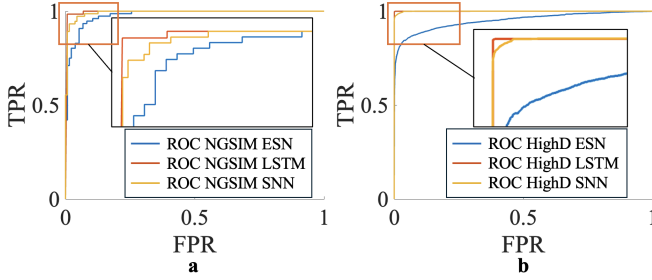


Fig. 5. ROC curves for SNN, LSTM, and ESN on the NGSIM (a) and HighD (b) datasets. The blue, red, and yellow curves represent the SNN, LSTM, and ESN methods, respectively.

The curves in Figure 5 are the ROC curves, which reflect the model's performance under different classification thresholds. The ROC curve plots the TPR against the FPR at various classification thresholds, and the area under the curve (AUC) is used to quantify the overall performance. A ROC curve closer to the top-left corner, with a higher AUC value, reflects better classification accuracy [30]. Figure 5a shows the ROC curves of the three methods on the NGSIM dataset. The AUC value of our method is 0.9925, the AUC value of the LSTM method is 0.9955, and the AUC value of the ESN method is the lowest at 0.9793. Figure 5b shows

the results on the HighD dataset. The AUC value of our method is 0.9994, the LSTM method achieves 0.9997, and the ESN method achieves 0.9503. These results demonstrate that our method performs excellently in prediction accuracy, achieving results comparable to the LSTM method while significantly outperforming the ESN method. Moreover, our method significantly outperforms the LSTM approach in terms of training efficiency, which underscores the advantage of our approach in effectively balancing both high accuracy and efficiency.

Then, as shown in Table I, our method has only 219 parameters, requires 0.01 MB of memory, converges in 375 s on the HighD dataset with an accuracy of 0.9828, and converges in 199 s on the NGSIM dataset with an accuracy of 0.9426. The ESN method has 1,503 parameters, requires 0.04 MB of memory, converges in 766 s on the HighD dataset with an accuracy of 0.8876, and converges in 276 s on the NGSIM dataset with an accuracy of 0.9043. The LSTM method, with 269,059 parameters and 80.81 MB of memory usage, achieves convergence in 1520 s on the HighD dataset with an accuracy of 0.9983, and in 796 s on the NGSIM dataset with an accuracy of 0.9809. These results demonstrate that our method significantly outperforms the ESN method in terms of parameters, memory usage, and training time while achieving high accuracy. Compared to the LSTM method, our approach offers substantial advantages in efficiency and resource utilization, with only a slight trade-off in accuracy.

In summary, the proposed method shows a compelling balance between accuracy and deployment efficiency. It not only delivers prediction performance comparable to LSTM but also demonstrates significant advantages in terms of resource consumption, training speed, and ease of deployment. Our approach is particularly well-suited for real-time applications and resource-limited environments, offering substantial benefits in both accuracy and deployment efficiency.

V. CONCLUSION

This paper proposes an efficient lane-changing intention prediction approach based on SNN, addressing the critical challenge of real-time and accurate prediction of surrounding vehicles' lane-changing behavior in autonomous driving systems. By leveraging the temporal dynamics and feature fusion capabilities of SNN, our method achieves high prediction accuracy while significantly improving training and deployment efficiency. The proposed approach reduces

TABLE I
COMPARISON OF MODELS ON HIGHD AND NGSIM DATASETS

Model	Dataset	Parameters	Memory Usage	Training Time	Accuracy
SNN	HighD	219	0.01 MB	375 s	0.9828
ESN	HighD	1,503	0.04 MB	766 s	0.8876
LSTM	HighD	269,059	80.81 MB	1520 s	0.9983
Model	Dataset	Parameters	Memory Usage	Training Time	Accuracy
SNN	NGSIM	219	0.01 MB	199 s	0.9426
ESN	NGSIM	1,503	0.04 MB	276 s	0.9043
LSTM	NGSIM	269,059	80.81 MB	796 s	0.9809

training time by 75% and memory usage by 99.9% compared to baseline methods, demonstrating its potential for practical deployment in resource-constrained environments. Experimental results show that, compared to LSTM and ESN methods, the proposed method achieves prediction accuracy comparable to LSTM and significantly outperforms ESN. In scenario validation, the proposed method accurately captures lane-changing timing, with the smallest deviation from actual lane-changing moments.

Future work will focus on optimizing the model architecture to improve both accuracy and efficiency. We will explore more scenarios to enhance the model's adaptability. Efforts will also be made to improve prediction performance in diverse conditions. Finally, we aim to test on real-world vehicles to validate the practical effectiveness.

ACKNOWLEDGMENT

This study is supported by RGC General Research Fund (GRF) HKUST16205224 and NSFC Grant U24A20252 and 62373315 and the Red Bird MPhil Program at the Hong Kong University of Science and Technology (Guangzhou)

REFERENCES

- [1] S. Mozaffari, O. Y. Al-Jarrah, M. Dianati, P. Jennings, and A. Mouzakitis, "Deep learning-based vehicle behavior prediction for autonomous driving applications: A review," *IEEE Transactions on Intelligent Transportation Systems*, vol. 23, no. 1, pp. 33–47, 2020.
- [2] A. Kesting, M. Treiber, and D. Helbing, "General lane-changing model mobil for car-following models," *Transportation Research Record*, vol. 1999, no. 1, pp. 86–94, 2007.
- [3] Q. Wang, Z. Li, and L. Li, "Investigation of discretionary lane-change characteristics using next-generation simulation data sets," *Journal of Intelligent Transportation Systems*, vol. 18, no. 3, pp. 246–253, 2014.
- [4] C. Ding, W. Wang, X. Wang, and M. Baumann, "A neural network model for driver's lane-changing trajectory prediction in urban traffic flow," *Mathematical Problems in Engineering*, vol. 2013, no. 1, p. 967358, 2013.
- [5] M. Shokrolah Shirazi and B. T. Morris, "Trajectory prediction of vehicles turning at intersections using deep neural networks," *Machine Vision and Applications*, vol. 30, pp. 1097–1109, 2019.
- [6] K. Griesbach, M. Beggato, and K. H. Hoffmann, "Lane change prediction with an echo state network and recurrent neural network in the urban area," *IEEE Transactions on Intelligent Transportation Systems*, vol. 23, no. 7, pp. 6473–6479, 2021.
- [7] D.-F. Xie, Z.-Z. Fang, B. Jia, and Z. He, "A data-driven lane-changing model based on deep learning," *Transportation research part C: emerging technologies*, vol. 106, pp. 41–60, 2019.
- [8] S. Ghosh-Dastidar and H. Adeli, "Third generation neural networks: Spiking neural networks," in *Advances in computational intelligence*. Springer, 2009, pp. 167–178.
- [9] S. Kundu, G. Datta, M. Pedram, and P. A. Beerel, "Spike-thrift: Towards energy-efficient deep spiking neural networks by limiting spiking activity via attention-guided compression," in *Proceedings of the IEEE/CVF winter conference on applications of computer vision*, 2021, pp. 3953–3962.
- [10] E. O. Neftci, H. Mostafa, and F. Zenke, "Surrogate gradient learning in spiking neural networks: Bringing the power of gradient-based optimization to spiking neural networks," *IEEE Signal Processing Magazine*, vol. 36, no. 6, pp. 51–63, 2019.
- [11] B. Rueckauer, I.-A. Lungu, Y. Hu, M. Pfeiffer, and S.-C. Liu, "Conversion of continuous-valued deep networks to efficient event-driven networks for image classification," *Frontiers in neuroscience*, vol. 11, p. 682, 2017.
- [12] R. Krajewski, J. Bock, L. Kloecker, and L. Eckstein, "The highd dataset: A drone dataset of naturalistic vehicle trajectories on german highways for validation of highly automated driving systems," in *2018 21st international conference on intelligent transportation systems (ITSC)*. IEEE, 2018, pp. 2118–2125.
- [13] B. Coifman and L. Li, "A critical evaluation of the next generation simulation (ngsim) vehicle trajectory dataset," *Transportation Research Part B: Methodological*, vol. 105, pp. 362–377, 2017.
- [14] W. Nelson, "Continuous-curvature paths for autonomous vehicles," in *Proceedings, 1989 International Conference on Robotics and Automation*. IEEE, 1989, pp. 1260–1264.
- [15] K. Liu, J. Gong, A. Kurt, H. Chen, and U. Ozguner, "Dynamic modeling and control of high-speed automated vehicles for lane change maneuver," *IEEE Transactions on Intelligent Vehicles*, vol. 3, no. 3, pp. 329–339, 2018.
- [16] M. Treiber and A. Kesting, "Modeling lane-changing decisions with mobil," in *Traffic and Granular Flow'07*. Springer, 2009, pp. 211–221.
- [17] R. S. Tomar, S. Verma, and G. S. Tomar, "Prediction of lane change trajectories through neural network," in *2010 International conference on computational intelligence and communication networks*. IEEE, 2010, pp. 249–253.
- [18] Y. Xing, C. Lv, H. Wang, D. Cao, and E. Velenis, "An ensemble deep learning approach for driver lane change intention inference," *Transportation Research Part C: Emerging Technologies*, vol. 115, p. 102615, 2020.
- [19] K. Griesbach, K. H. Hoffmann, and M. Beggato, "Prediction of lane change by echo state networks," *Transportation research part C: emerging technologies*, vol. 121, p. 102841, 2020.
- [20] H. Zhang and R. Fu, "Target vehicle lane-change intention detection: An approach based on online transfer learning," *Computer Communications*, vol. 172, pp. 54–63, 2021.
- [21] H. Fang, A. Shrestha, and Q. Qiu, "Multivariate time series classification using spiking neural networks," in *2020 International Joint Conference on Neural Networks (IJCNN)*. IEEE, 2020, pp. 1–7.
- [22] Y. Kim and P. Panda, "Optimizing deeper spiking neural networks for dynamic vision sensing," *Neural Networks*, vol. 144, pp. 686–698, 2021.
- [23] L. Deng, Y. Wu, X. Hu, L. Liang, Y. Ding, G. Li, G. Zhao, P. Li, and Y. Xie, "Rethinking the performance comparison between snns and anns," *Neural networks*, vol. 121, pp. 294–307, 2020.
- [24] A. Sengupta, Y. Ye, R. Wang, C. Liu, and K. Roy, "Going deeper in spiking neural networks: Vgg and residual architectures," *Frontiers in neuroscience*, vol. 13, p. 95, 2019.
- [25] A. Viale, A. Marchisio, M. Martina, G. Masera, and M. Shafique, "Carsnn: An efficient spiking neural network for event-based autonomous cars on the loihi neuromorphic research processor," in *2021 International Joint Conference on Neural Networks (IJCNN)*. IEEE, 2021, pp. 1–10.
- [26] J. López-Randulfe, T. Duswald, Z. Bing, and A. Knoll, "Spiking neural network for fourier transform and object detection for automotive radar," *Frontiers in Neurobotics*, vol. 15, p. 688344, 2021.
- [27] Z. Bing, C. Meschede, G. Chen, A. Knoll, and K. Huang, "Indirect and direct training of spiking neural networks for end-to-end control of a lane-keeping vehicle," *Neural Networks*, vol. 121, pp. 21–36, 2020.
- [28] S. Jokhio, P. Olleja, J. Bärghman, F. Yan, and M. Baumann, "Analysis of time-to-lane-change-initiation using realistic driving data," *IEEE Transactions on Intelligent Transportation Systems*, 2023.
- [29] J. N. Mandrekar, "Receiver operating characteristic curve in diagnostic test assessment," *Journal of Thoracic Oncology*, vol. 5, no. 9, pp. 1315–1316, 2010.
- [30] L. E. Moses, D. Shapiro, and B. Littenberg, "Combining independent studies of a diagnostic test into a summary roc curve: data-analytic approaches and some additional considerations," *Statistics in medicine*, vol. 12, no. 14, pp. 1293–1316, 1993.